Forensic Sciences Research, 2025, Vol. 10, Issue 3
https://doi.org/10.1093/fsr/owaf002
Research Article

A novel signal processing approach enabled by machine learning for the detection and identification of chemical warfare agent simulants using a GC-QEPAS system

Nicola Liberatore[1], Giorgio Felizzato[2,*], Sandro Mengali[1], Roberto Viola[1] and Francesco Saverio Romolo[2]

[1]Consorzio CREO, L'Aquila, Italy
[2]Department of Law, University of Bergamo, Bergamo, Italy

*Corresponding author. E-mail: giorgio.felizzato@unibg.it

Abstract

The detection and identification of chemical warfare agents (CWAs) present challenges in emergency response scenarios and for safety and security applications. This study presents the development and validation of an innovative analytical method using a gas chromatography (GC) and quartz-enhanced photoacoustic spectroscopy (QEPAS) sensor for the detection of stimulants for six CWAs. Following the guidelines of the European Network of Forensic Science Institute (ENFSI) and the Commission Implementing Regulation (EU) 2021/808, the analytical method was validated. The validation results demonstrated the robustness and reliability of both the GC and QEPAS modules. Moreover, with regard to the toxicological threshold levels, this study highlights the efficacy of a prototype of a portable device for real security and safety applications. Furthermore, a machine learning (ML) approach was developed to automate the detection and identification of CWAs' stimulants. The workflow involved two interconnected stages: detection based on chromatographic retention times (RTs), and identification using infrared (IR) spectra through the one-class support vector machines classifier. The classifier was activated only after obtaining a positive detection based on RTs. The results highlight the ML model's effectiveness in CWA detection and identification, combining RT analysis and IR spectrum classification, achieving 97% accuracy at a 95.5% confidence interval and 99% accuracy at a 99.7% confidence interval; this result demonstrates the model's utility for real-world security and safety applications for CWAs.

Keywords: forensic sciences; machine learning; chemical warfare agents; chemical weapons; gas chromatography; quartz enhanced photoacoustic spectroscopy

Introduction

According to the Chemical Weapons Convention, chemical weapons (CWs) are defined as "toxic chemicals and their precursors, munitions and devices, specifically designed to cause death or other harm" [1]. These extremely toxic chemicals are also known as chemical warfare agents (CWAs), which can be dispersed as a gas, liquid, aerosol, or agent adsorbed to particles to produce either lethal or incapacitating effects on humans [2].

The first to respond to an attack involving CWAs is likely the police, fire department, and emergency medical personnel. When the incident does not raise immediate awareness, healthcare specialists are likely the first to be involved in treating the victims. First, operators need to identify the contaminated area, which is called the "hot zone" [3]. Moreover, it is important to identify—in a timely manner—the chemical compound used in the attack to provide the best cure for the victims [4]. Therefore, portable analytical devices are the most important analytical tools in CWA scenarios, as they enable a prompt identification of both the hot zone and the compound(s) used.

In the last few years, many efforts have been made to develop portable analytical instruments for on-site analysis, characterized by their high accuracy, sensitivity, and prompt response. Among such methods, colourimetric assays are easy to use, fast, and cheap in terms their capability to detect different types of CWAs by changing colours in the presence of the analytes [5]. Moreover, gold nanoparticles have been studied to improve the detection of CWAs in both colourimetric and fluorescence assays [6–8]. The gas phase detection of CWAs has been investigated through various portable devices, such as portable Raman [9], electronic nose system based on surface acoustic wave (SAW) sensors [10, 11], a portable gas-sensing instrument based on an MEMS-fabricated micropreconcentrator (μPC) coupled with a film bulk acoustic resonator (FBAR) gas sensor [12], and broadband photoacoustic spectroscopy [13]. Ion mobility spectrometers (IMS) have also been proven to be effective with CWAs [14]. Moreover, gas chromatography (GC) coupled with IMS has been used to separate the sample into individual components prior to detection, thereby enhancing chemical identification within complex matrices [15]. In recent years, various chemoresistive

Received: June 13, 2024. **Accepted:** January 16, 2025
© The Author(s) 2025. Published by OUP on behalf of the Academy of Forensic Science.
This is an Open Access article distributed under the terms of the Creative Commons Attribution Non-Commercial License (https://creativecommons.org/licenses/by-nc/4.0/), which permits non-commercial re-use, distribution, and reproduction in any medium, provided the original work is properly cited. For commercial re-use, please contact journals.permissions@oup.com

Downloaded from https://academic.oup.com/fsr/article/10/3/owaf002/7964709 by guest on 31 October 2025

gas sensors have been studied due to their potentially high selectivity and fast response times. Despite these advantages, there remain challenges in their fabrication and functional characterization. Consequently, many improvements in this field are necessary before chemoresistive gas sensors can be effectively used as commercial analytical devices [16, 17].

For surface analysis, various devices have been developed, such as a portable capillary electrophoretic system with contactless conductometric detection used for the *in situ* analysis of extracted samples [18]. Laser-induced breakdown spectroscopy (LIBS) has also been employed for detecting surface contamination by CWAs [19].

Different analytical devices based on mass spectrometry (MS) have been developed, including membrane inlet mass spectrometric technology integrated onto a portable system [20] and a portable mass spectrometer equipped with an electron cyclotron resonance ion source (mini ECRIS-MS) used for *in situ* monitoring of trace amounts of CWAs in atmospheric air [21]. Moreover, GC–MS instrumentation for field analysis [22], including a palm portable mass spectrometer [23], has been demonstrated to be useful for the detection and identification of CWAs.

In this article, we present a sensing scheme based on GC and quartz-enhanced photoacoustic infrared spectroscopy (QEPAS), recently developed by CREO, which has demonstrated its effectiveness in detecting and identifying CWA simulants. This technology has shown reliable detection and identification capabilities for HAZMAT compounds—including CWA simulants such as dimethyl-methylphosphonate (DMMP), di-propylene-glycol-methyl-ether (DPGME), and methyl salicylate as well as the actual CWA yperite and drug precursors—even in the presence of strong interferents at concentrations much higher than the targeted hazardous compounds [24–26].

Compared to sensors described in the scientific literature, GC-QEPAS offers numerous advantages. The QEPAS module uses a quartz tuning fork to detect the photoacoustic signal generated by the absorption of light by gas molecules, providing extremely high sensitivity and selectivity. These characteristics are crucial for identifying CWAs, which are extremely dangerous even in small concentrations. Additionally, the QEPAS detector offers a fast response and, thus, enables real-time monitoring of gas concentrations. The GC module further enhances the system's selectivity by separating complex mixtures into individual components, reducing false positives, and improving the identification of specific CWAs.

The integration of these two modules into a portable, compact, and reliable sensing solution makes GC-QEPAS highly competitive with existing sensors. While colourimetric assays are cheap and easy to use, they generally lack the sensitivity and specificity needed to detect trace levels of CWAs in complex environments. Raman devices offer portable solutions, but often suffer from lower sensitivity and higher susceptibility to interferents compared to GC-QEPAS. In comparison with GC-IMS and GC–MS, GC-QEPAS aims to be less prone to false alarms and memory effects than the former, less complex, less bulky, and easier to transport where analysis is needed.

Further, the GC-QEPAS sensor provides sizeable quantities of multivariate data in the form of chromatograms and infrared (IR) spectra. Multivariate analysis and other statistical methods are crucial to process large datasets and enhance the usability of database information and spectroscopic outputs [27]. Machine learning (ML) is a part of artificial intelligence (AI) defined as "the set of all tasks in which a computer can make decisions based on data" [28] and it is used to teach the machines how to handle the data more efficiently [29]. In addition, the synergy between ML and spectroscopy provides a fast, useful, and efficient solution for analyzing samples of interest both for industrial and research applications [30]. Studies have revealed that ML techniques can significantly improve the extraction of valuable information from spectral data, thereby creating unprecedented opportunities for advancements in analytical science [31]. For these reasons, an ML method based on IR spectra was utilized in this article. Among all the ML methods, multiclass classification allows users to classify an unknown sample into one of many pre-defined categories. In contrast, one-class classification enables the identification of samples that belong to a specific class from all possibilities by training a classifier exclusively on a target dataset [32, 33]. A large number of one-class classifiers have been proposed in the literature. One-class support vector machines (OC-SVMs) have been demonstrated to be effective in many articles [34–36] owing to their robustness, effective handling of high-dimensional data sets, and flexibility in defining the boundary of normal data points. For these reasons, the OC-SVMs were selected to be studied in this article as part of developing an automated detection and identification process to enable the use of the sensor in on-site applications.

In this study, the novel GC-QEPAS sensor was used to analyze three more CWA simulants for the first time and to develop and validate an analytical method to enable the detection and identification of chemical warfare agent simulants on-site. Moreover, the study aimed to develop an automated classification model for real-world applications of that sensor by employing a one-class ML approach in order to extract useful insights from spectral data.

Materials and methods

GC-QEPAS sensor (or instrumentation)

GC is the golden-standard analytical method for the separation of components in a gas mixture [37]. QEPAS is one of several techniques of spectroscopy that enables the detection and identification of gases and vapors by means of the measurement of their absorption spectra [38]. Moreover, compared to other techniques, QEPAS stands out for its particularly low interrogation volume, which allows optimal coupling with micro GC devices for the creation of compact, robust, and fast sensors. The GC-QEPAS sensor developed by CREO consists of three modules: a compact first stage for gas sampling and preconcentration of large air volumes, a fast GC (FAST-GC) module for chemical separation of the gas sample, and a QEPAS module for chemical analysis.

The sampling and preconcentration module is a compact purge and trap device based on commercial sorbent tubes from Markes International Ltd., which allows to sample approximately one liter of air and desorb the preconcentrated vapors into the FAST-GC separation module in less than 3 min.

The FAST-GC module is a compact GC developed by CNR-IMM (Bologna, Italy) [39], comprising one MEMS for preconcentration and injection and one MEMS for the GC column for separation implemented on a silicon micromachined chip.

Downloaded from https://academic.oup.com/fsr/article/10/3/owaf002/7964709 by guest on 31 October 2025

The analysis module is a QEPAS detector, which enables the measurement of the photoacoustic spectra of the analytes eluted by the FAST-GC module. The QEPAS module utilizes a quantum cascade laser source (MiniQCL; Block Engineering, Southborough, MA, USA), which can continuously scan the thermal IR spectrum in the range of wavelengths between 7.4 mm and 10.7 mm to perform spectroscopic analysis.

The QEPAS sensor is equipped with a mini-PC controller to automatically manage all the sensing chains and run the spectral analysis algorithms for identification.

A more detailed description of each module of the GC-QEPAS sensor has been reported in our previous paper [24]. Here, we only recall the sensing scheme of the system, which is illustrated in Figure 1: a given volume of air is sucked up by the sampling and preconcentration module; the MEMS preconcentration cartridge captures sampled vapors; the fast desorption and injection of the captured mix into the MEMS chromatographic column allows for the separation of the different components of the mix; each component of the mix that exits the column is analyzed by the QEPAS module, which enables the acquisition of infrared spectra.

The main parameters of the setting that were applied to each module of the GC-QEPAS sensor for the validation with simulants of CWAs are reported in Supplementary Table S1.

Reagents and analytical methodology

In this study, a selection of six CWAs were analyzed: mustard gas simulants—methyl salicylate (CAS 119–36-8) [40], diethyl sulfide (DES, CAS 352–93-2) [41], DPGME (CAS 34590–94-8) [42]; and sarin simulants—dimethyl-methyl phosphonate (DMMP, CAS 756–79-6) [43, 44], diethyl methyl phosphonate (DEMP, CAS 683–08-9) [45], and trimethyl phosphonate (TMP, CAS 512–56-1) [46]. The molecular structures of the tested chemical compounds and the corresponding CWA are presented in Figure 2.

All the target analytes—methyl salicylate, DES, DPGME, DMMP, DEMP, and TMP—were purchased from Monforte Lab Suppliers (Grassobbio, Italy).

In order to replicate a real environmental scenario with controlled concentrations of target analytes, a 60-L glass chamber was utilized and connected to the sensor sampler by a plastic tube. Samples were introduced into the chamber by puncturing a porous septum positioned at the top of the box, using a 10-μL syringe (Eppendorf, Hamburg, Germany). Below the septum, a hot crucible was installed to facilitate sample evaporation. To prevent sample decomposition, the temperature of the hot crucible was carefully regulated to ensure it was sufficiently high to improve the vaporization of the analytes without causing thermal degradation. The average temperature used for this purpose was ∼40°C. Moreover, the results obtained using the hot crucible were compared with analyses conducted without it (both the retention time and the shape of the IR curve) to ensure that sample degradation was avoided. The IR curves were compared by using Pearson's correlation coefficient. Consequently, a well-known concentration of analytes was achieved within the chamber. Figure 3 depicts the sample injection into the chamber using a syringe and an enlargement of the hot crucible.

Multivariate data analysis was performed using Python code within a Jupyter Notebook environment. The following packages were used in the modules: NumPy [47], Pandas [48], Matplot library [49], Plotly [50], and Scikit-Learn [51]. The data and code used for this work are shared and can be freely accessed at https://github.com/giorgiofelizzato/GC-QEPAS-chemical-warfare-agents.

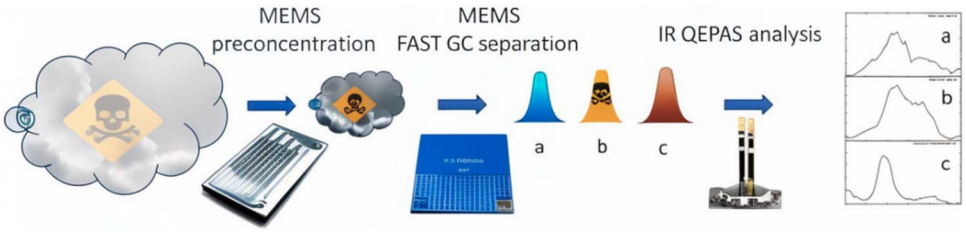

Figure 1 Sensing scheme of the GC-QEPAS sensor. MEMS: micro-electromechanical systems; IR: infrared; QEPAS: quartz enhanced photoacoustic spectroscopy.

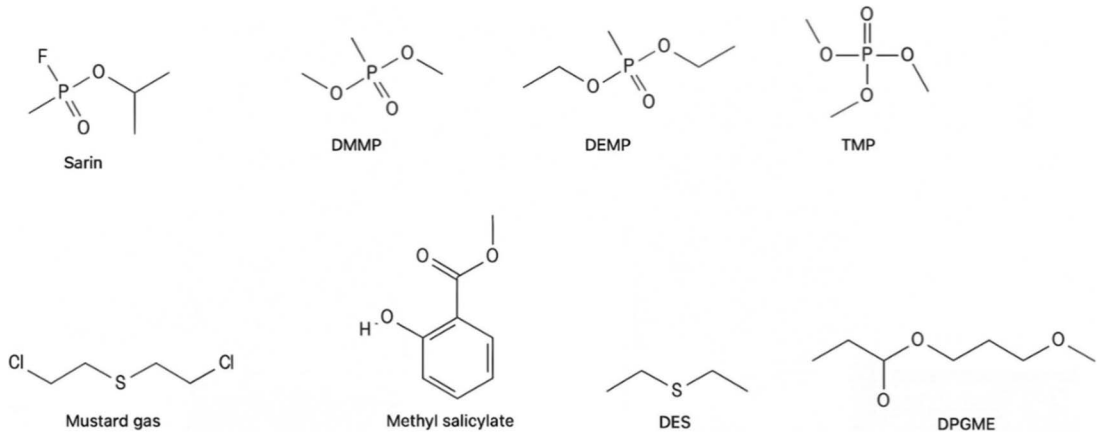

Figure 2 Target analyte chemical structures. DMMP: dimethyl methyl phosphonate; DEMP: diethyl methyl phosphonate; TMP: trimethyl phosphonate; DES: diethyl sulfide; DPGME: dipropylene glycol methyl ether.

Downloaded from https://academic.oup.com/fsr/article/10/3/owaf002/7964709 by guest on 31 October 2025

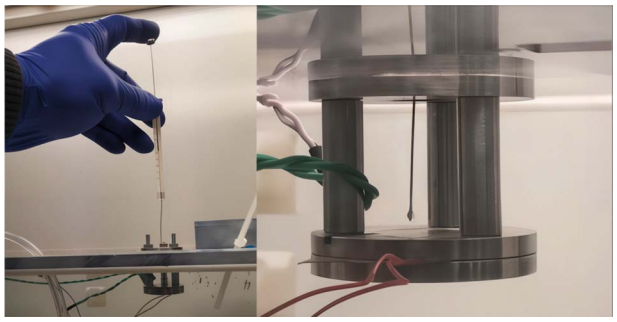

Figure 3 The injection of the sample into the chamber using a syringe (A) and the hot crucible positioned below the septum, used to facilitate the sample evaporation (B).

Validation

Validation was performed according to the European Network of Forensic Science Institute (ENFSI) guidelines and the Commission Implementing Regulation (EU) 2021/808 based on a validation plan for qualitative methods [52, 53]. Based on these, the following validation parameters were considered: limit of detection (LoD), repeatability, and within-laboratory reproducibility.

The LoD is the lowest concentration detectable with statistical significance through the specific analytical procedure. LoD values were experimentally estimated by considering three times the signal-to-noise (SN) ratio of the recorded chromatographs [52, 54].

Repeatability is defined as the precision under the same operating conditions, where independent test results are obtained using the same method, in the same laboratory, and by the same operator using the same equipment within short intervals of time. Repeatability was calculated both for the chromatographic outputs (retention time, RT) and the IR spectrum, using the standard deviation and the coefficient of variation (CV%) of the retention time and the position of the maximum value in the spectrum. Further, repeatability was calculated based on at least six replicates of the analysis of each target analyte, performed on the same day, and in the same experimental conditions, such as room temperature, batch of solvents, and operator [52].

Within-laboratory reproducibility was calculated both for the chromatographic outputs (RT) and the IR spectrum. For the chromatographic outputs, the standard deviation and the coefficient of variation (CV) of the RTs were evaluated. For the IR spectra, the position of the maximum of the spectra was assessed by using the standard deviation and the percentage of the CV. Reproducibility was calculated based on at least 18 replicates of the analysis of each target analyte, split over at least three different days (six replicates for each day) with different operators, different batches of reagents and solvents, and different room temperatures and ambient moisture [52].

Results and discussion

The abovementioned validation parameters were independently calculated for both the GC and QEPAS modules to ensure the generation of reliable data from all the components of the sensor.

Chromatogram peaks were represented as Gaussian curves using the probability density function (PDF) in Figure 4 [55]. Each peak or Gaussian curve is characterized by the average RT (the center of the peak) and the corresponding standard deviation, which defines the width of the curve. The majority of target analytes are well separated from each other, as depicted in Supplementary Table S2 and graphically in Figure 4. However, the peaks of TMP and DEMP are partially overlapping. The overlap between the two Gaussian distributions was quantified by calculating the area under the curve (AUC) shared by the peaks of the two chemical compounds. Numerically, the overlap between the Gaussian distributions is estimated to be 10%, thereby indicating that 10% of the area under the curve is shared between the two distributions.

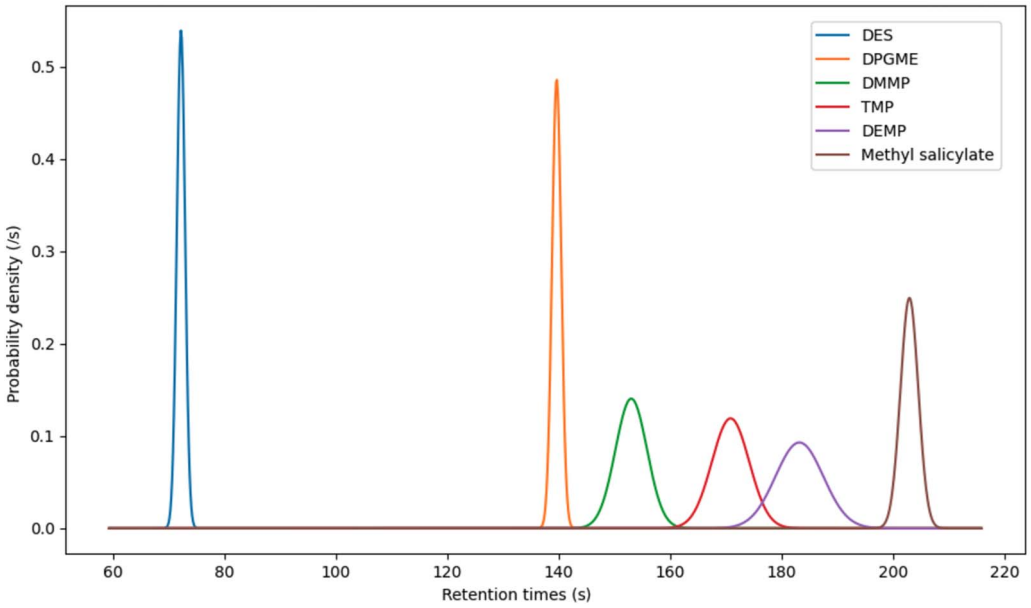

Figure 4 The probability density functions of the Gaussian distributions of target analytes. DES: diethyl sulfide; DPGME: dipropylene glycol methyl ether; DMMP: dimethyl methyl phosphonate; TMP: trimethyl phosphonate; DEMP: diethyl methyl phosphonate.

Downloaded from https://academic.oup.com/fsr/article/10/3/owaf002/7964709 by guest on 31 October 2025

In addition, the LoD was estimated. DMMP showed the lowest LoD among the target analytes, measuring 0.007 ppm. Moreover, repeatability and within-laboratory reproducibility were calculated for the GC module based on the CV% of RTs. The results on repeatability were lower than 1% for DPGME and methyl salicylate, while it was close to 1% for DES. DMMP and TMP had a CV% of close to 2% and DEMP had a CV% of slightly above 2%. The results are summarized in Table 1.

The CV of retention time was taken into account to evaluate the within-laboratory reproducibility. All the analytes indicated a CV% of lower than 4%. The results are summarized in Table 2.

Following the aforementioned procedures, the validation protocol was employed to validate the QEPAS module that produces the IR spectra. Variations in the positions of the maximum of the spectra were evaluated for each target analyte for repeatability and within-laboratory reproducibility, thereby ensuring reliable results across multiple measurements and different experimental conditions. The CV% for repeatability was consistently below 0.5% for all analytes. Notably, for two analytes—DES and methyl salicylate—it was not possible to determine any variation (both recorded at 0.00% rounded to two decimal values). Similar results were obtained for within-laboratory reproducibility. The CV% for all analytes, except DEMP, remained below 0.5%. DEMP exhibited a CV% close to 2%, while methyl salicylate continued to have a CV% of 0.00%. The results are summarized in Tables 3 and 4.

The overall validation protocol highlights the excellent repeatability and within-laboratory reproducibility of analytical results obtained by both the GC and the QEPAS modules. The RTs recorded for the different target analytes have been demonstrated to be repeatable and reproducible. The final outputs have not been significantly affected by employing different operators and experimental conditions.

The QEPAS module underwent the same validation protocol to ensure reliable outputs. The CV for each target analyte confirms reliability in repeatability and within-laboratory reproducibility. Consequently, the analytical method is considered effective for its intended use and can be utilized in real scenarios for reliable detection and identification of chemical warfare agent simulants.

The suitability of the instrument sensitivity was evaluated considering the toxicity of the CWAs discussed in the article. The toxicity of a vapor or aerosol chemical agent can be assessed using Acute Exposure Guideline Levels (AEGLs), which delineate the airborne concentrations above which individuals—including vulnerable subpopulations such as children and the elderly—may experience distinct adverse health effects. AEGLs are categorized based on the severity of the effects: AEGL-1 indicates levels causing notable discomfort or irritation, AEGL-2 denotes concentrations leading to serious and long-lasting health effects, and AEGL-3 represents life-threatening risks or potential death. AEGLs are commonly expressed in mg/m^3 or ppm. These guideline levels are established for five exposure periods: 10 and 30 min as well as 1, 4, and 8 h [56]. The AEGL values are presented in Supplementary Table S3 [57].

Considering the LoD achieved for the simulants of sarin and mustard gas, the analytical method has been demonstrated to be effective in detecting and identifying CWAs in real-world scenarios, which is a crucial capability for safety and security applications. Specifically, all mustard gas simulants discussed in this study exhibited LoDs lower than the AEGL-3 for a 4-h exposure period, thereby ensuring the detection of life-threatening risks or potential fatalities. Additionally, the LoD for DPGME was lower than the AEGL-3 for an 8-h exposure, further enhancing the method's capability of detecting critical risks. Furthermore, the LoD for DES was found to be lower than the AEGL-2 for a 10-min exposure and equivalent to the AEGL-2 for a 30-min exposure, thereby indicating the method's effectiveness in recognizing concentrations associated with long-lasting health effects. On the other hand, the LoD of DMMP, a sarin simulant, was lower than AEGL-3 for an exposure of 8 h. Consequently, all the potential risks of fatalities would be recognized. Moreover, the LoD of DMMP is lower than AEGL-2 for an exposure of 30 min,

Table 1. Limit of detection and repeatability for the GC outputs.

Target analyte	LoD (ppm)	Average RT (s)	Std. Dev. RT (s)	CV% RT
DES	0.090	72.16	0.74	1.00
DPGME	0.030	139.6	0.82	0.58
DMMP	0.007	153.0	2.80	1.90
TMP	0.017	170.8	3.40	2.00
DEMP	0.068	183.2	4.30	2.30
Methyl salicylate	0.160	202.9	1.60	0.79

GC: gas chromatography; DES: diethyl sulfide; DPGME: dipropylene glycol methyl ether; DMMP: dimethyl methyl phosphonate; TMP: trimethyl phosphonate; DEMP: diethyl methyl phosphonate; LoD: limit of detection; RT: retention time; Std. Dev: standard deviation; CV%: coefficient of variation.

Table 2. Within-laboratory reproducibility for the GC outputs.

Target analyte	Average RT (s)	Std. Dev. RT (s)	CV% RT
DES	72.3	1.8	2.5
DPGME	137.6	4.1	3.0
DMMP	149.1	5.5	3.7
TMP	168.8	5.2	3.3
DEMP	183.5	4.4	2.4
Methyl salicylate	199.6	5.1	2.5

GC: gas chromatography; DES: diethyl sulfide; DPGME: dipropylene glycol methyl ether; DMMP: dimethyl methyl phosphonate; TMP: trimethyl phosphonate; DEMP: diethyl methyl phosphonate; LoD: limit of detection; RT: retention time; Std. Dev: standard deviation; CV%: coefficient of variation.

Downloaded from https://academic.oup.com/fsr/article/10/3/owaf002/7964709 by guest on 31 October 2025

Table 3. Repeatability for QEPAS spectra.

Target analyte	Average peak position (maximum of the spectrum) (μm)	Std. Dev. (mm) peak position	CV% peak position
DES	8.00	0.00	0.00
DPGME	8.92	0.02	0.18
DMMP	9.50	0.02	0.16
TMP	9.41	0.03	0.31
DEMP	9.55	0.01	0.11
Methyl salicylate	8.18	0.00	0.00

QEPAS: quartz enhanced photoacoustic spectroscopy; DES: diethyl sulfide; DPGME: dipropylene glycol methyl ether; DMMP: dimethyl methyl phosphonate; TMP: trimethyl phosphonate; DEMP: diethyl methyl phosphonate; LoD: limit of detection; RT: retention time; Std. Dev.: standard deviation; CV%: coefficient of variation.

Table 4. Within-laboratory reproducibility for QEPAS spectra.

Target analyte	Average peak position (maximum of the spectrum) (μm)	Std. Dev. (mm) peak position	CV% peak position
DES	8.02	0.03	0.04
DPGME	8.89	0.02	0.02
DMMP	9.50	0.04	0.37
TMP	9.42	0.03	0.03
DEMP	9.52	0.18	1.90
Methyl salicylate	8.18	0.00	0.00

QEPAS: quartz enhanced photoacoustic spectroscopy; DES: diethyl sulfide; DPGME: dipropylene glycol methyl ether; DMMP: dimethyl methyl phosphonate; TMP: trimethyl phosphonate; DEMP: diethyl methyl phosphonate; LoD: limit of detection; RT: retention time; Std. Dev.: standard deviation; CV%: coefficient of variation.

thereby providing a reliable method to recognize the concentration of a few long-lasting health effects. This comprehensive analysis emphasizes the analytical method's robustness in detecting and identifying CWAs in various exposure scenarios.

Machine learning classification

The workflow was structured into two sections that were interconnected: the first stage focused on the *detection* based on the chromatographic RTs, while the second aimed at the *identification* of CWA simulants based on the entire IR spectra by a one-class ML classifier. The automated module was designed to exclusively employ the ML classifier when a positive detection based on chromatographic RTs is obtained. A sample is classified into a specific class when it is positively detected by means of the RT and positively classified by the one-class ML model using IR data.

Detection by using retention time

The GC module of the sensor enables the separation of individual components within a complex mixture, thereby providing an RT for each compound detected. The chromatograms are generated by considering the total absorption spectrum across the entire IR scanning range at each retention time. By analyzing the same target compounds multiple times, it was possible to calculate the average RT and the related standard deviation. These statistical parameters were used to represent the chromatography peaks as Gaussian curves by using the PDFs, as depicted in Figure 3.

For real cases, the PDF model was applied to detect CWAs in the environment around the sensor. For a positive detection, the following two confidence intervals were tested:

95.5% (corresponding to $2 \times std.dev$ of the Gaussian curve) and a higher confidence interval of 99.7% (corresponding to $3 \times std.dev$ of the Gaussian curve).

Whenever the retention time of an unknown compound falls within the confidence extreme values, a positive detection is given. The 99.7% confidence interval reduces the likelihood of false negatives, but may lead to more false positives.

An example is presented in Figure 5. In the example, a compound with a retention time of 140.22 s is identified as DPGME.

When the value of the retention time is within the confidence interval (values presented in Supplementary Table S4), a positive detection is obtained, as in the example, the automated ML model is employed to identify the specific CWA simulant. By employing a confidence level of three standard deviations, the range of RTs increases. Consequently, this expanded range encompasses more variation among RTs, thereby leading to a lower number of false negatives but simultaneously to a higher number of false positives because more compounds are likely to have an RT that falls within this range.

One-class support vector machines

The entire IR spectra provided by the QEPAS module underwent the standard normal variate pre-processing, which centered and scaled each spectrum by the corresponding standard deviation in order to reduce the multiplicative effects of scattering [58]. Figure 6 presents an example of the DMMP IR spectrum acquired by QEPAS.

Subsequently, OC-SVMs were used as a one-class ML classifier based on the entire pre-processed IR spectra. One-class classification aims to identify and categorize a specific class of objects while distinguishing them from all other potential objects. The classifier efficiently categorizes the target objects (inlier) and treats any others as outliers [59]. When a compound is classified as an inlier by the OC-SVM, it implies that the compound's characteristics match those of the target compounds used to set up the model. Consequently, the compound can be successfully identified.

Downloaded from https://academic.oup.com/fsr/article/10/3/owaf002/7964709 by guest on 31 October 2025

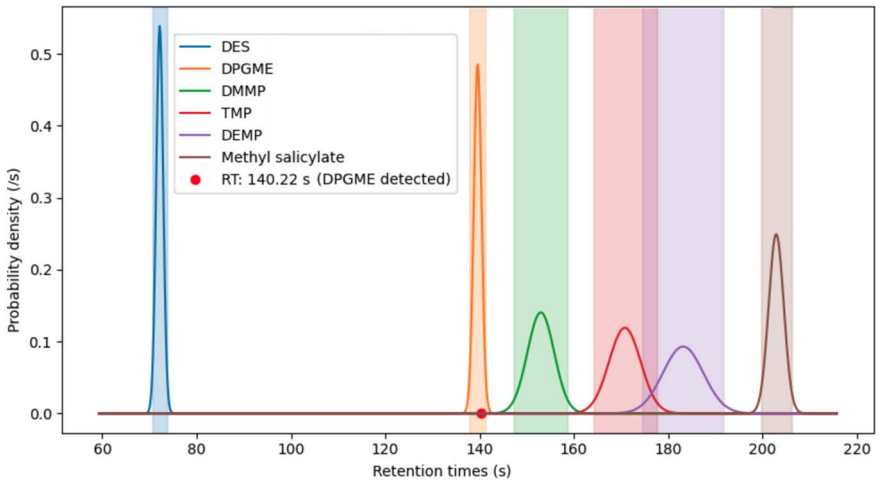

Figure 5 Probability density functions compared with ranges of two times the standard deviation. DES: diethyl sulfide; DPGME: dipropylene glycol methyl ether; DMMP: dimethyl methyl phosphonate; TMP: trimethyl phosphonate; DEMP: diethyl methyl phosphonate.

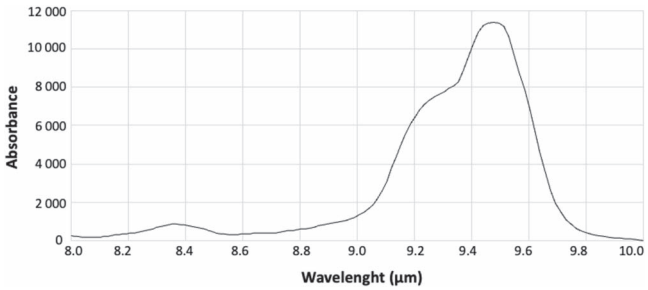

Figure 6 Infrared spectrum of dimethyl methyl phosphonate.

For each CWA simulant, a one-class SVM classifier was developed and its parameters were optimized. Four kernels were taken into account to build the classifier: linear, radial basis function, polynomial, and sigmoidal. In the case of the polynomial kernel, different degrees were considered to maximize the model accuracy. Each classifier's optimal kernel for real-world applications was determined based on minimizing misclassifications.

The ML approach employed in this study offers significant advantages over the correlation coefficient methods, which typically involve comparing the experimental spectrum with a theoretical one [60]. OC-SVM was selected for several reasons, particularly its robustness in handling anomaly data and outliers inherent in spectral analysis, such as noise and measurement differences in acquired spectra. During the training phase of our OC-SVM model, we deliberately incorporated various experimental conditions, batches of reagents, concentrations, and various operators. This approach reflects real-world scenarios and also introduces challenges for traditional correlation coefficient methods. Correlation coefficients are sensitive to variations like different backgrounds or SN ratios and frequently provide misleading results or false positives due to their linear nature and susceptibility to noise. Moreover, the OC-SVM requires only the data of the target class during training. In contrast, the use of correlation coefficients would typically require access to theoretical spectra for all target substances, often sourced from databases including spectra acquired with various types of analytical instruments.

Finally, the ML approach was comprehensively assessed taking into account the accuracy of each classifier. *Leave-p-out cross-validation* (LPO) was selected as the leading method to evaluate the models' performance in this article. LPO randomly splits the original dataset into a training set—used to set up the model) and an evaluation set (used to assess the model's performance) [61]. In this study, 70% of the dataset was used as the training set, while the remaining 30% was used as the evaluation set. The accuracy of each OC-SVM classifier was used as the evaluating parameter.

The model validation included both the detection by means of the RTs using the PDF and the OC-SVM for the identification of the CWA simulant. Supplementary Table S5 presents the kernel used for each simulant and the overall model accuracy taking into account the two confidence intervals (Supplementary Table S5) for the detection: 95.5% and 99.7% of the PDF Gaussian curves obtained using the RTs.

The overall model accuracy achieved with a 95.5% confidence interval for GC detection was 97%. Conversely, using a 99.7% confidence interval for detection, the overall accuracy increased to 99%. This comprehensive evaluation highlights the effectiveness of the ML approach in detecting and identifying CWA simulants based on both RTs and IR spectra.

Conclusion

This study explored and demonstrated the effectiveness of the novel GC-QEPAS prototype developed by CREO for the detection and identification of CWAs. The analytical method developed to detect and identify six simulants of sarin and mustard gas was validated according to the EENFSI and Commission Implementing Regulation (EU) 2021/808. Throughout the validation process, the performance of both the GC and QEPAS modules was evaluated, considering their repeatability, within-laboratory reproducibility, and the LoD. The LoD of the analytical method was assessed in terms of the toxicological properties of CWAs involved in this study, considering the AEGLs. The LoD obtained for the simulants of sarin and mustard gas was lower than the AEGL-2 and AEGL-3 for both the mentioned CWAs. This comprehensive assessment confirmed the suitability for qualitative analysis in real scenarios of safety and security applications.

Downloaded from https://academic.oup.com/fst/article/10/3/owaf002/7964709 by guest on 31 October 2025

In addition, an ML methodology was developed to detect and identify CWA simulants in real-world scenarios. The ML approach involved two key sections: the detection by means of the RTs and the identification through the OCl-SVM classifier applied to IR spectra. When a positive detection was made, the corresponding IR spectrum was analyzed by the OC-SVM classifier to provide a classification as an inlier or outlier. Consequently, the compound can be successfully identified when its characteristics match those of the target compounds used to establish the model. By employing two different confidence intervals for the detection, 95.5% and 99.7%, overall model accuracy values of 97% and 99%, respectively, were obtained. Thus, the employed classification method was proven to be effective for forensic applications.

Authors' contributions

Nicola Liberatore, Giorgio Felizzato and Francesco Saverio Romolo were responsible for the study's conceptualization and methodology. Data collection was handled by Nicola Liberatore, Roberto Viola and Sandro Mengali, while all authors contributed to data analysis and interpretation. Software development was led by Nicola Liberatore, Giorgio Felizzato, Roberto Viola and Sandro Mengali. Nicola Liberatore and Giorgio Felizzato drafted the manuscript, with all authors involved in reviewing and editing. Visualization was managed by Nicola Liberatore, Giorgio Felizzato and Roberto Viola. Project supervision was provided by Sandro Mengali and Francesco Saverio Romolo. Sandro Mengali and Francesco Saverio Romolo handled project administration, and all authors contributed resources. All authors reviewed and approved the final manuscript.

Compliance with ethical standards

This article does not contain any studies with human participants or animals performed by any of the authors.

Disclosure statement

No conflict of interest is declared by the authors.

Funding

This research received funding from the European Union's Horizon 2020 research and innovation programme under grant agreement [No 883116, RISEN project].

References

1. Chemical Weapons Convention. Convention on the Prohibition of the Development, Production, Stockpiling and Use of Chemical Weapons and on their Destruction. Paris; 1993.
2. Ganesan K, Raza SK, Vijayaraghavan R. Chemical warfare agents. J Pharm Bioallied Sci. 2010;2:166–178.
3. Fish JT, Stout RN, Wallace E. Practical Crime Scene Investigations for Hot Zones. 1st ed., vol. 52. Boca Raton (FL): CRC Press; 2010.
4. World Health Organization (WHO). Public Health Response to Biological and Chemical Weapons: WHO Guidance. Geneva: WHO; 2004.
5. Kangas MJ, Burks RM, Atwater J, et al. Colourimetric sensor arrays for the detection and identification of chemical weapons and explosives. Crit Rev Anal Chem. 2017;47:138–153.
6. Yue G, Su S, Li N, et al. Gold nanoparticles as sensors in the colourimetric and fluorescence detection of chemical warfare agents. Coord Chem Rev. 2016;311:75–84.
7. Zhang S, Swager TM. Fluorescent detection of chemical warfare agents: functional group specific ratiometric chemosensors. J Am Chem Soc. 2003;125:3420–3421.
8. Dagnaw FW, Cai YP, Song QH. Rapid and sensitive detection of nerve agent mimics by *meso*-substituted BODIPY piperazines as fluorescent chemosensors. Dyes Pigm. 2021;189:109257.
9. Lafuente M, Sanz D, Urbiztondo M, et al. Gas phase detection of chemical warfare agents CWAs with portable Raman. J Hazard Mater. 2020;384:121279–121279.
10. Matatagui D, Martí J, Fernández MJ, et al. Optimized design of a SAW sensor array for chemical warfare agents simulants detection. Procedia Chemistry. 2009;1:232–235.
11. Matatagui D, Martí J, Fernández MJ, et al. Chemical warfare agents simulants detection with an optimized SAW sensor array. Sens Actuators B. 2011;154:199–205.
12. Yan X, Qu H, Chang Y, et al. A prototype portable instrument employing micro-preconcentrator and FBAR sensor for the detection of chemical warfare agents. Nanotechnol Precis Eng Cheng. 2022;5:43–48.
13. Mikkonen T, Luoma D, Hakulinen H, et al. Detection of gaseous nerve agent simulants with broadband photoacoustic spectroscopy. J Hazard Mater. 2022;440:129851.
14. Yamaguchi S, Asada R, Kishi S, et al. Detection performance of a portable ion mobility spectrometer with ^{63}Ni radioactive ionization for chemical warfare agents. Forensic Toxicol. 2010;28:84–95.
15. Erickson RP, Tripathi A, Maswadeh WM, et al. Closed tube sample introduction for gas chromatography–ion mobility spectrometry analysis of water contaminated with a chemical warfare agent surrogate compound. Anal Chim Acta. 2006;556:455–461.
16. Barreca D, Maccato C, Gasparotto A. Metal oxide nanosystems as chemoresistive gas sensors for chemical warfare agents: a focused review. Adv Mater Interfaces. 2022;9.14:2102525.
17. Barreca D, Gasparotto A, Gri F, et al. Plasma-assisted growth of β-MnO_2 nanosystems as gas sensors for safety and food industry applications. Adv Mater Interfaces. 2018;5.23:1800792.
18. Kubáň P, Seiman A, Makarõtševa N, et al. *In situ* determination of nerve agents in various matrices by portable capillary electropherograph with contactless conductivity detection. J Chromatogr A. 2011;1218:2618–2625.
19. L'Hermite D, Vors E, Vercouter T, et al. Evaluation of the efficacy of a portable LIBS system for detection of CWA on surfaces. Environ Sci Pollut Res Int. 2016;23:8219–8226.
20. Virgen CA, Fox JD, Santariello P, et al. Portable membrane inlet mass spectrometric detection and analysis of chemical warfare agent simulants at the U.S. Army Dugway Proving Ground S/K challenge event. Int J Mass Spectrom. 2021;468:116635.
21. Urabe T, Takahashi K, Kitagawa M, et al. Development of portable mass spectrometer with electron cyclotron resonance ion source for detection of chemical warfare agents in air. Spectrochim Acta A Mol Biomol Spectrosc. 2014;120:437–444.
22. Smith PA, Koch D, Hook GL, et al. Detection of gas-phase chemical warfare agents using field-portable gas chromatography–mass spectrometry systems: instrument and sampling strategy considerations. TrAC Trends Anal Chem. 2004;23:296–306.
23. Yang M, Kim TY, Hwang HC, et al. Development of a palm portable mass spectrometer. J Am Soc Mass Spectrom. 2008;19:1442–1448.
24. Zampolli S, Mengali S, Liberatore N, et al. A MEMS-enabled deployable trace chemical sensor based on fast gas-chromatography and quartz enhanced photoacoustic spectroscopy. Sensors. 2020;20:120.
25. Liberatore N, Viola R, Mengali S, et al. Compact GC-QEPAS for on-site analysis of chemical threats. Sensors (Basel). 2023;23:270.
26. Viola R, Mengali S, Libetatore N, et al. Deployable sensor for trace identification of hazardous chemicals in dirty environment, based

Downloaded from https://academic.oup.com/fsr/article/10/3/owaf002/7964709 by guest on 31 October 2025

on FAST gas-chromatography and quartz enhanced photoacoustic spectroscopy. In: Proceedings of the PhotonIcs & Electromagnetics Research Symposium—Spring (PIERS-Spring); 2019 Jun 17–20. Rome, Italy, 2019. p. 223–28.
27. European Network of Forensic Science Institutes Drugs Working Group. Guideline for the use of chemometrics in forensic chemistry. Finland. ENFSI; 2020.
28. Serrano L. Grokking machine learning. Shelter Island (NY): Simon and Schuster. 2021.
29. Batta M. Machine learning algorithms—a review. Int J Sci Res. 2020;9:381–386.
30. Ramírez CAM, Greenop M, Ashton L, et al. Applications of machine learning in spectroscopy. Appl Spectrosc Rev. 2021;56: 733–763.
31. Qi Y, Hu D, Jiang Y, et al. Recent progresses in machine learning assisted Raman spectroscopy. Adv Opt Mater. 2023; 11.14:2203104.
32. Oza P, Patel VM. One-class convolutional neural network. IEEE Signal Process Lett. 2019;26:277–281.
33. Deng X, Li W, Liu X, et al. One-class remote sensing classification: one-class *vs*. binary classifiers. Int J Remote Sens. 2018;39: 1890–1910.
34. Wang E, Wang ZY, Wu Q. One novel class of Bézier smooth semi-supervised support vector machines for classification. Neural Comput Applic. 2021;33:9975–9991.
35. Tian J, Gu H, Gao C, et al. Local density one-class support vector machines for anomaly detection. Nonlinear Dyn. 2011;64: 127–130.
36. Lesouple J, Baudoin C, Spigai M, et al. How to introduce expert feedback in one-class support vector machines for anomaly detection? Signal Process. 2021;188:108197.
37. Harold MN, Miller JM, Snow NH. Basic gas chromatography. Hoboken (NJ): Wiley & Sons; 2009.
38. Kosterev AA, Dong L, Thomazy D, et al. QEPAS for chemical analysis of multi-component gas mixtures. Appl Phys B. 2010;101: 649–659.
39. Zampolli S, Elmi I, Cardinali GC, et al. Compact-GC platform: a flexible system integration strategy for a completely microsystems-based gas-chromatograph. Sens Actuators B Chem. 2020;305:127444.
40. James T, Wyke S, Marczylo T, et al. Chemical warfare agent simulants for human volunteer trials of emergency decontamination: a systematic review. J Appl Toxicol. 2018;38:113–121.
41. Montoro C, Linares F, Quartapelle Procopio E, et al. Capture of nerve agents and mustard gas analogues by hydrophobic robust MOF-5 type metal–organic frameworks. J Am Chem Soc. 2011;133:11888–11891.
42. Bigiani L, Zappa D, Barreca D, et al. Sensing nitrogen mustard gas simulant at the ppb scale *via* selective dual-site activation at Au/Mn_3O_4 interfaces. ACS Appl Mater Interfaces. 2019;11: 23692–23700.
43. Zheng Q, Fu YC, Xu JQ. Advances in the chemical sensors for the detection of DMMP—a simulant for nerve agent sarin. Procedia Eng. 2010;7:179–184.
44. Bielecki M, Witkiewicz Z, Rogala P. Sensors to detect sarin simulant. Crit Rev Anal Chem. 2021;51:299–311.
45. Mathieu O, Kulatilaka WD, Petersen EL. Shock-tube studies of sarin surrogates. Shock Waves. 2019;29:441–449.
46. Senyurt EI, Schoenitz M, Dreizin EL. Rapid destruction of sarin surrogates by gas phase reactions with focus on diisopropyl methylphosphonate (DIMP). Def Technol. 2021;17:703–714.
47. Harris CR, Millman KJ, van der Walt SJ, et al. Array programming with NumPy. Nature (London). 2020;585:357–362.
48. The Pandas Development Team. Pandas: Data Analysis Library [software] Version 1.0.2020.
49. Hunter JD. Matplotlib: a 2D graphics environment. Comput Sci Eng. 2007;9:90–95.
50. Plotly Technologies Inc. Collaborative data science [software]. Montréal (QC): Plotly Technologies Inc.; 2015.
51. Pedregosa F, Varoquaux G, Gramfort A, et al. Scikit-learn: machine learning in python. J Mach Learn Res. 2011;12:2825–2830.
52. European Network of Forensic Science Institutes (ENFSI). Guidelines for the single laboratory validation of instrumental and human based methods in forensic science. 2014.
53. European Commission. Commission Implementing Regulation (EU) 2021/808 of 22 March 2021on the performance of analytical methods for residues of pharmacologically active substances used in food-producing animals and on the interpretation of results as well as on the methods to be used for sampling and repealing Decisions 2002/657/EC and 98/179/EC. Off J Eur Union. 2021;2180:84–108.
54. Konieczka P. Validation and regulatory issues for sample preparation. In: Comprehensive sampling and sample preparation: analytical techniques for scientists. Vol 2. Oxford (UK): Elsevier. 2012;2: 699–711.
55. Li J, Xingkai Y. Survey on information fusion of probability density functions. Aero Weaponry. 2023;30:1–10. Chinese.
56. Bruckner JV, Keys DA, Fisher JW. The acute exposure guideline level (AEGL) program: applications of physiologically based pharmacokinetic modeling. J Toxicol Environ Health A. 2004;67: 621–634.
57. National Research Council of the National Academies. Acute exposure guideline levels for selected airborne chemicals. vol. 3. Washington, DC: National Academies Press; 2000.
58. Bi Y, Yuan K, Xiao W, et al. A local pre-processing method for near-infrared spectra, combined with spectral segmentation and standard normal variate transformation. Anal Chim Acta. 2016;909: 30–40.
59. Shin HJ, Eom DH, Kim SS. One-class support vector machines—an application in machine fault detection and classification. Comput Ind Eng. 2005;48:395–408.
60. Samuel AZ, Mukojima R, Horii S, et al. On selecting a suitable spectral matching method for automated analytical applications of Raman spectroscopy. ACS Omega. 2021;6:2060–2065.
61. Liu S. Leave-*p*-out cross-validation test for uncertain verhulst-Pearl model with imprecise observations. IEEE Access. 2019;7: 131705–131709.

Downloaded from https://academic.oup.com/fsr/article/10/3/owaf002/7964709 by guest on 31 October 2025

© The Author(s) 2025. Published by OUP on behalf of the Academy of Forensic Science. This is an Open Access article distributed under the terms of the Creative Commons Attribution Non-Commercial License (https://creativecommons.org/licenses/by-nc/4.0/), which permits non-commercial re-use, distribution, and reproduction in any medium, provided the original work is properly cited.
For commercial re-use, please contact journals.permissions@oup.com
Forensic Sciences Research, 2025, Vol. 10, Issue 3
https://doi.org/10.1093/fsr/owaf002
Research Article